Electronic Supplementary Material (ESI) for Physical Chemistry Chemical Physics.

Microfluidic Study of Synergic Liquid-Liquid Extraction of Rare Earth Elements

Asmae El Maangar[1,2]. Johannes Theisen[1]. Christophe Penisson[1]. Thomas Zemb[2]. and Jean-Christophe P. Gabriel[1,3,*,†]

[1] Institut de Chimie Séparative de Marcoule (ICSM). CEA/CNRS/UM2/ENSCM. F-38054. University Grenoble Alpe. CEA. Grenoble

[2] Institut de Chimie Séparative de Marcoule (ICSM). CEA/CNRS/UM2/ENSCM. F-30207. Bagnols-sur-Cèze

[3] Nanoscience and Innovation for Materials. Biomedecine and Energy (NIMBE). CEA/CNRS/Univ. Paris-Saclay. CEA Saclay. F-91191 Gif-sur-Yvette

* Corresponding authors: JCP Gabriel (jean-christophe.gabriel@cea.fr)

[†] Current address: Energy Research Institute @ NTU (ERI@N). Nanyang Technology University. Singapore.

1 Supplementary Materials:

1.1. Sample preparation

Table 1: Corresponding molar concentrations of the two extractants used for constant total concentration 0.9 mol.L^{-1} for several DMDOHEMA molar fractions.

$X_{DMDOHEMA}$	**0**	**0.25**	**0.5**	**0.75**	**1**
[HDEHP] **(mol/L)**	0.9	0.675	0.45	0.225	0
[DMDOHEMA] **(mol/L)**	0	0.225	0.45	0.675	0.9

1.2.Microfluidic system:

Table 2: Contact time and the corresponding applied flow rate.

CONTACTE TIME **(MIN)**	FLOW RATE **(µL/MIN)**
1	34.00
3	11.33
10	3.40
30	1.13
60	0.57

1.3.Extraction efficiency versus time

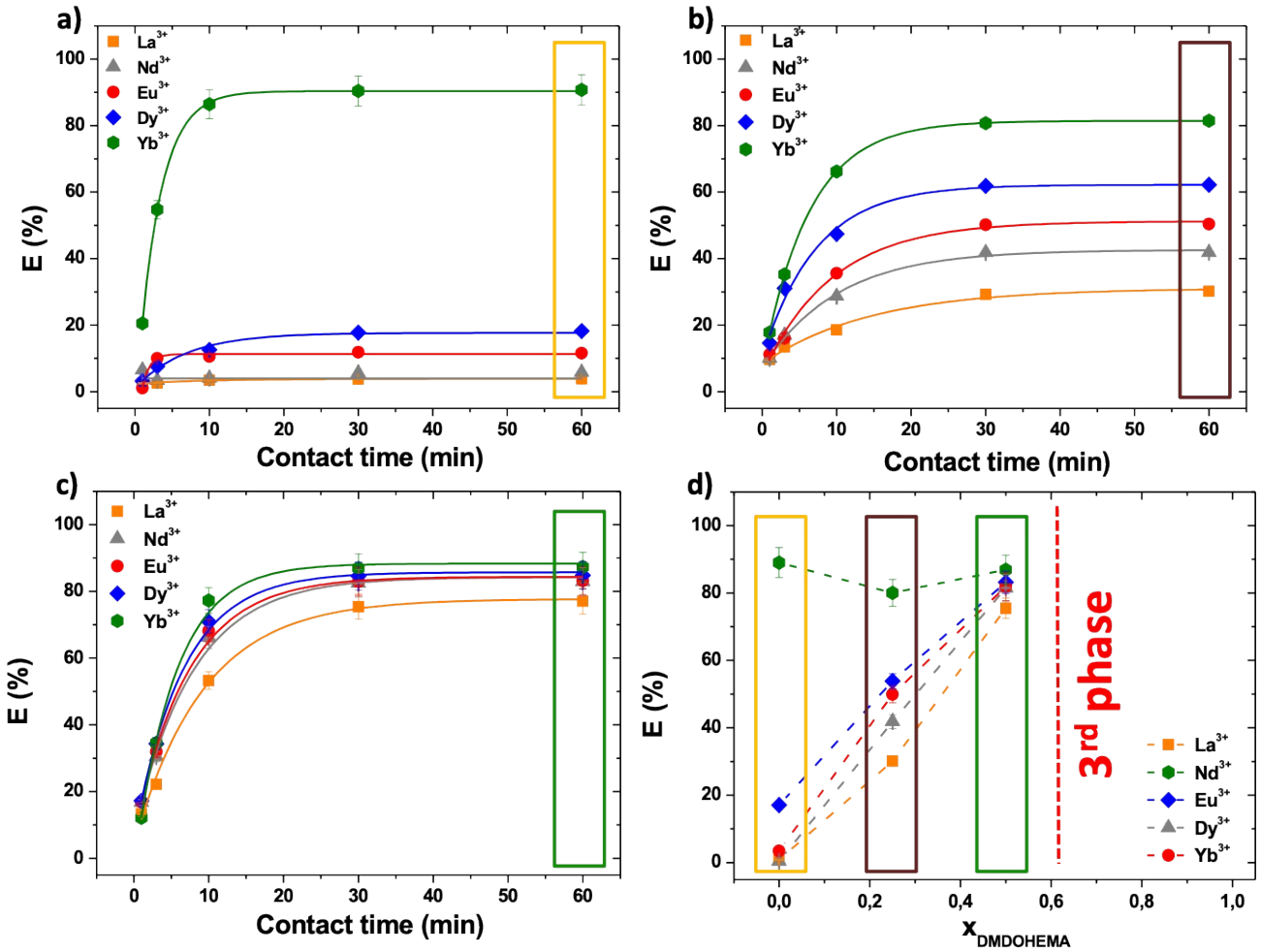

Figure 1: (a)-(c) raw data of the extraction efficiency versus time obtained in microfluidics for different lanthanides (La^{3+}. Nd^{3+}. Eu^{3+}. Dy^{3+}. Yb^{3+}) and molar fractions of DMDOHEMA. [HNO_3] = 0.3M. T = 25°C. $x_{DMDOHEMA}$ = 0 (a); 0.25 (b); 0.5 (c). Coherence with values obtained via a standard batch method after 1h of extraction is shown in figure (d).

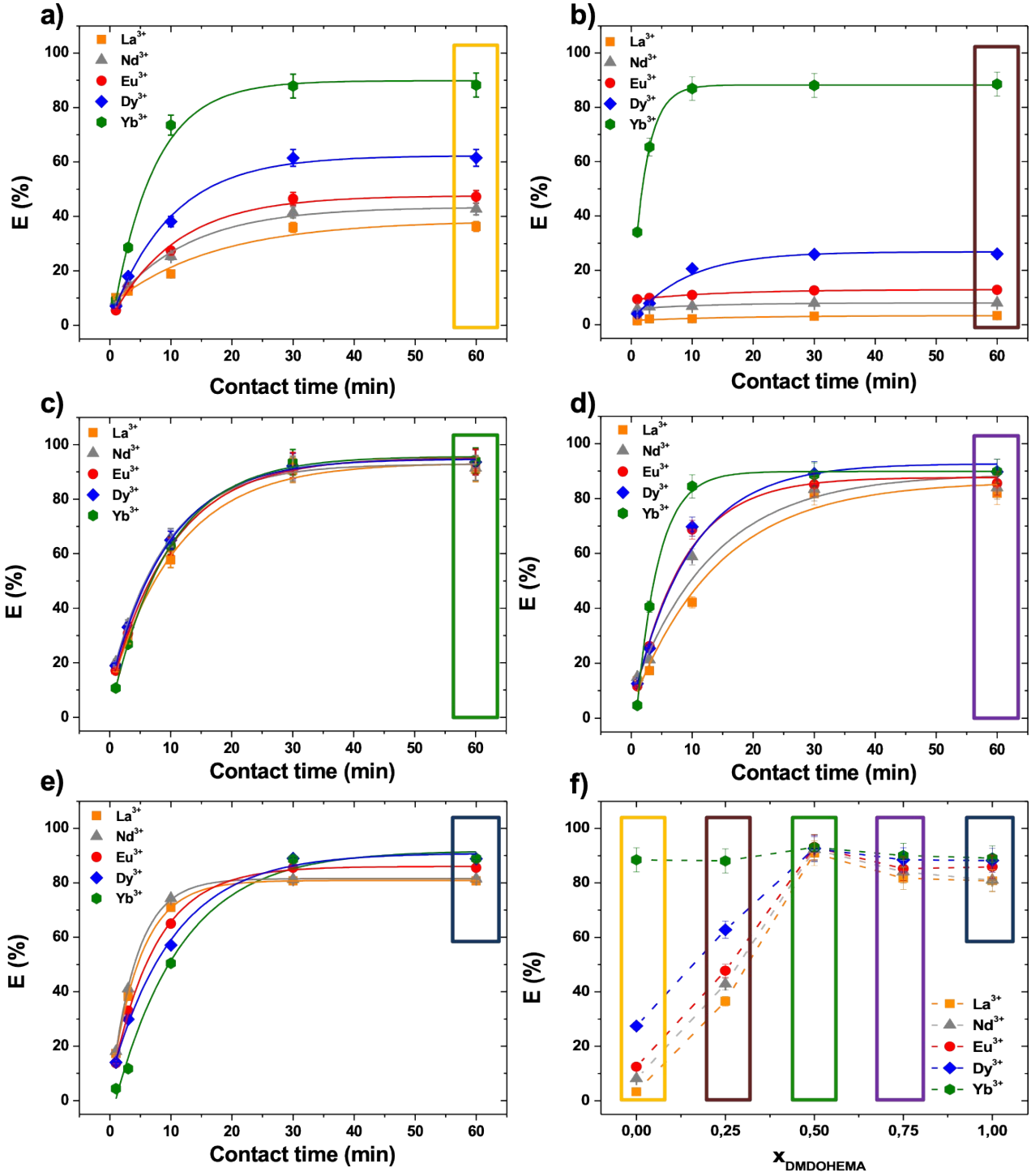

Figure 2: (a)-(e) raw data of the extraction efficiency versus time obtained in microfluidics for different lanthanides (La^{3+}. Nd^{3+}. Eu^{3+}. Dy^{3+}. Yb^{3+}) and molar fractions of DMDOHEMA. [HNO_3] = 3M. T = 25°C. $x_{DMDOHEMA}$ = 0 (a). 0.25 (b). 0.5 (c). 0.75 (d). 1 (e). Coherence with equilibrium (1h) values obtained via a standard batch method is shown as figure (f).

Table 3: the difference of the extraction ratio between batch and microfluidics (%) for different lanthanides (La^{3+}. Nd^{3+}. Eu^{3+}. Dy^{3+}. Yb^{3+}) and molar fractions of DMDOHEMA (0. 0.25. 0.5. 0.75. 1). [HNO_3] = 0.3 M. T = 25°C

$x_{DMDOHEMA}$	La	Nd	Eu	Dy	Yb
0.00	0.0307	0.0543	0.0811	0.0114	0.0172
0.25	0.0008	0.0000	0.0052	0.0836	0.0144
0.50	0.0161	0.0141	0.0130	0.0163	0.0043

Table 4: the difference of the extraction ratio between batch and microfluidics (%) for different lanthanides (La^{3+}. Nd^{3+}. Eu^{3+}. Dy^{3+}. Yb^{3+}) and molar fractions of DMDOHEMA (0. 0.25. 0.5. 0.75. 1). [HNO_3] = 3 M. T = 25°C

$x_{DMDOHEMA}$	La	Nd	Eu	Dy	Yb
0.00	0.0000	0.0014	0.0033	0.0145	0.0001
0.25	0.0024	0.0014	0.0056	0.0130	0.0014
0.50	0.0007	0.0084	0.0043	0.0097	0.0103
0.75	0.0022	0.0011	0.0032	0.0128	0.0017
1.00	0.0002	0.0048	0.0038	0.0064	0.0020

1.4. Free energy of transfer versus acid concentration:

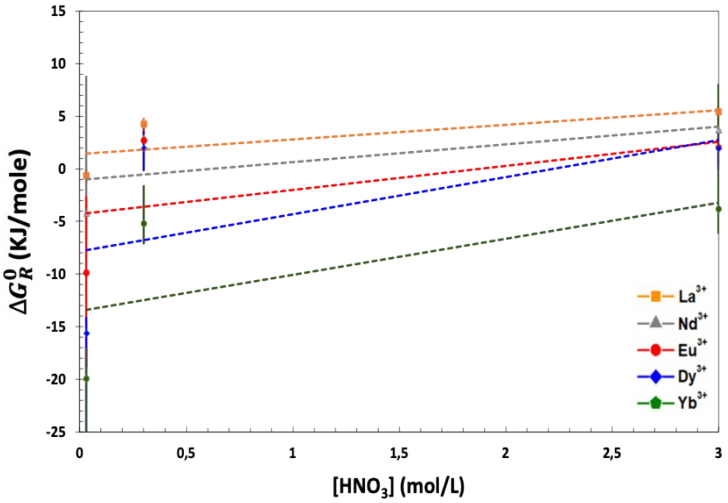

Figure 3 : Free energies of transfer ΔG (kJ/mole) versus HNO_3 concentration for HDEHP extractant ($x_{DMDOHEMA}$=0) T=25°C.

1.5. Precision in determination of free energy of transfer

The free energy of ion transfer between organic and aqueous phases can be determined by measuring the concentrations of rare earth elements in both of them using off-line X-ray fluorescence measurements. In order to calculate these concentrations with their associated errors, a new method was developed which is explained hereafter.

It relies on generating a full spectrum with the best secondary target according to composition. Then, a PLS (Partial least square) algorithm is used to defined a regression matrix from samples of known concentrations.[1-5] Thus, concentrations from unknown samples can be extracted thanks to this regression matrix. Moreover, there is a known

external constraint that can be used in the determination of the ratio of extracted and non-extracted species: the sum of the atoms present within the two outgoing fluids must be equal to the amount within the incoming fluid. Adding this external constraint means minimizing the uncertainty in the distribution coefficient.

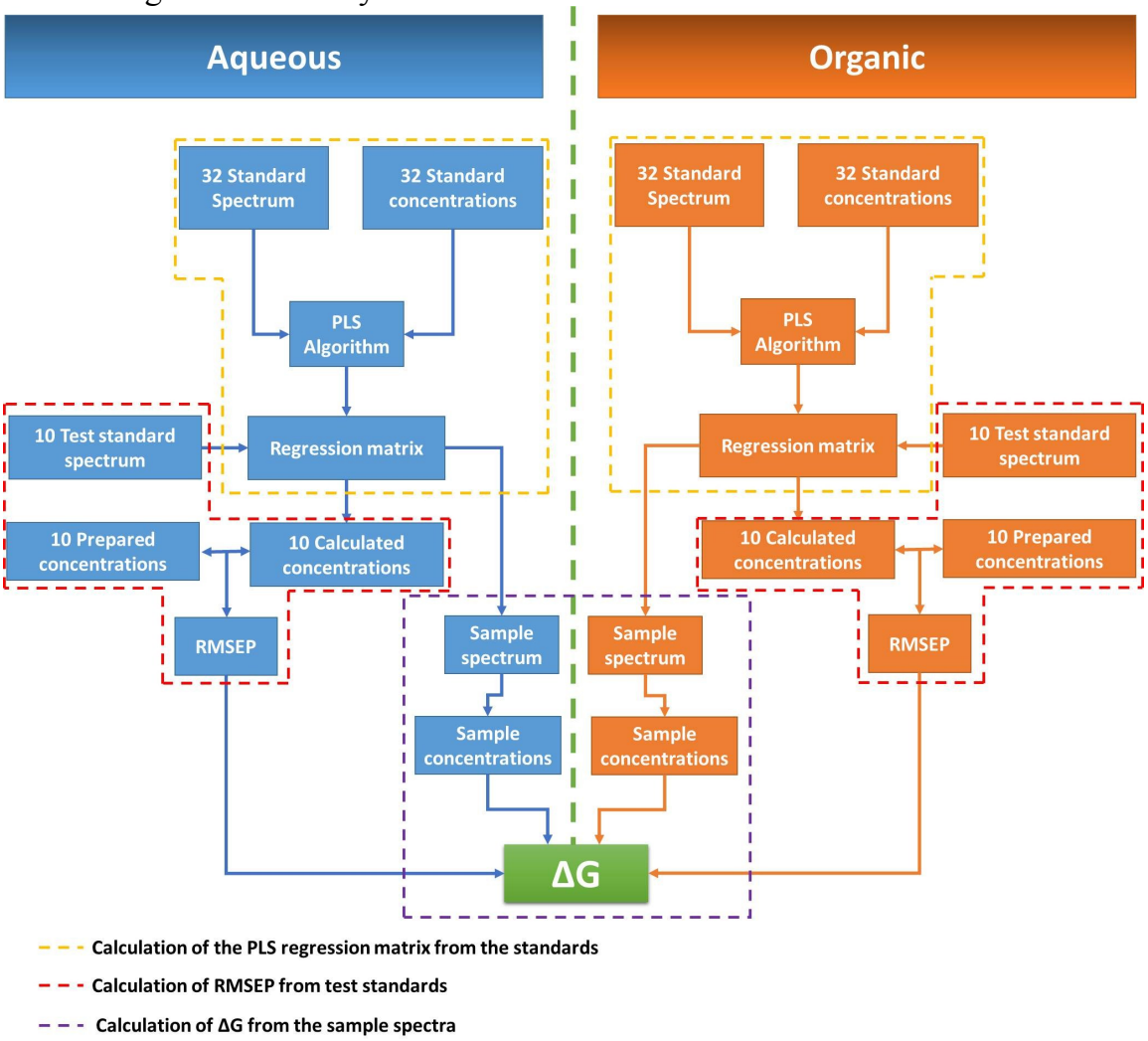

Figure 4: scheme of the different steps of the spectral treatment program to obtain the free energy of transfer and its associated error.

The exact procedure for obtaining the free energy of transfer using the XRF (as described in detail by Penisson)[6] is summarized in the Figure 4 and can be divided into 3 main steps:

1. The calculation of the regression matrix from samples prepared with known concentrations in both the aqueous and organic phases: the program provided by Kirsanov et al. was used to define 42 secondary standard samples to be prepared at varying concentrations of five lanthanides: La, Nd, Eu, Dy, Yb and Iron.[4] These samples were prepared from 75 mmol/L stock aqueous solutions of corresponding lanthanide nitrates in 3 M nitric acid. Lanthanide concentrations were varied in a range from 0.2 to 12.5 mmol.L^{-1}. The lower limit of the range is chosen at the limit of quantification estimated by the signal-to-noise ratio of the lanthanum peak. The upper limit is defined above the maximum ion concentration of solutions of interest to be studied. This concentration range was relevant and adapted for liquid-liquid

extractions studied in the laboratory using microfluidics. The system to study is composed of an aqueous phase in a nitric medium containing La, Nd, Eu, Dy, Yb and Fe at a concentration of 10 mmol.L^{-1} and an organic phase containing the extractant diluted in Isane IP175. The preparation of stock solutions in the case of organic standards was prepared by liquid-liquid extraction. The aqueous phases were prepared by dilution of nitrates salts of lanthanides and iron weighed whereas the organic phases were prepared by weighing the extracting molecule HDEHP diluted in Isane IP175. The organic phases prepared were contacted for one hour at 25°C in tubes placed horizontally and shaken planetary. Then, the phases were separated by centrifugation at 15025 G for 10 minutes. The values of the extracted cations concentrations were measured by ICP. Finally, the dilutions of the mother phases were carried out with micropipettes. The 84 samples prepared were measured with the SPECTRO XRF spectrometer to obtain the regression matrices which are calculated from the 32 standards.

2. The calculation of the root mean squared error of prediction: The matrices obtained are then tested with the remaining 10 standard samples that are used as independent test sets to assess the predictive power of the calibration model by calculating the Root Mean Square of Error Prediction (RMSEP) which gives information on the measurement error by comparing the concentrations measured by the PLS algorithm with those prepared. It can be calculated as follows:

$$RMSEP = \sqrt{\sum_{i=1}^{n} \frac{\left(c_i^{PLS} - c_i^{prep}\right)^2}{n}} \qquad \text{Equation 1}$$

Where c_i^{PLS} is a lanthanide concentration value derived from the PLS. c_i^{prep} is the actual lanthanide concentration and n is the number of samples.

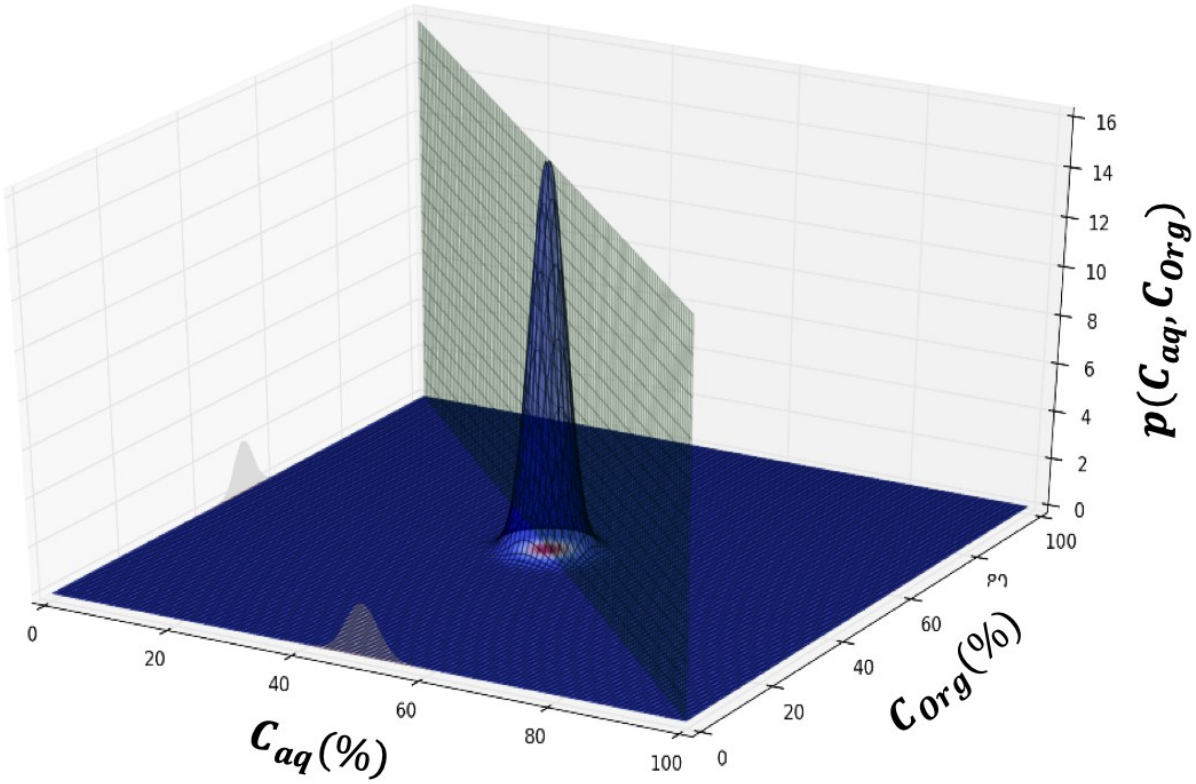

Figure 5 : 3D representation of probability with the mass conservation plan

3. The calculation of the free energy of transfer ΔG: A new method was used to calculate the transfer energies from the concentrations in the two extraction phases and their associated errors. The probability of measurement can be represented by a two-dimensional Gaussian function of the corresponding concentrations and standard deviations (Equation 2) which can be traced in three-dimensional space as a function of both the concentration in water and oil (Figure 5).

$$p(C_{aq}.C_{org}) = \frac{1}{2\pi\,\sigma_{aq}\sigma_{org}}\, e^{-\frac{1}{2}\left[\left(\frac{C_{aq} - C^{mesure}_{aq}}{\sigma_{aq}}\right)^2 + \left(\frac{C_{org} - C^{mesure}_{org}}{\sigma_{org}}\right)^2\right]} \qquad \text{Equation 2}$$

Where: σ_{aq} is the standard deviation on aqueous concentrations and σ_{org} is the standard deviation on organic concentrations

Now, since we know that during a liquid liquid extraction the total concentration of ions remains constant, in the defined three-dimensional domain, this property is translated by a plane that the 2D Gaussian should cut at its centre. In reality, the measurement has some uncertainty and the point ($Caq.\ Corg$) will not coincide exactly to this plane. In this case, the most probable energy of transfer value will be at the intersection between the plane and the 2D Gaussian. To determine the most probable transfer energy, the intersection curve between the plane and the 2D Gaussian is calculated. The maximum probability corresponds to the most probable

ΔG. The error is defined by the width at half height. Note that this is the reason why we do not obtain symmetrical error bars as shown in Figure 6 and Figure 7

Overall, this method uses the concentrations of ions in the two phases and the law of conservation of mass to determine the most probable energy of transfer and the associated errors. From this paragraph we can now understand why XRF with the adequate minimization procedure is the most precise method for obtaining chemical potentials. Typically, with 10% uncertainty. Especially that the use of tracers in nanomole quantities are relying on complex safety procedure and absorption problems that are hard to control. On the other hand, the standard ICP-OES requires back-extraction to measure organic phase concentrations, and is therefore relying on yet another chemical step, adding to the experimental error. Only XRF has the dynamic range and selectivity for immediate analysis and even direct coupling whenever possible.

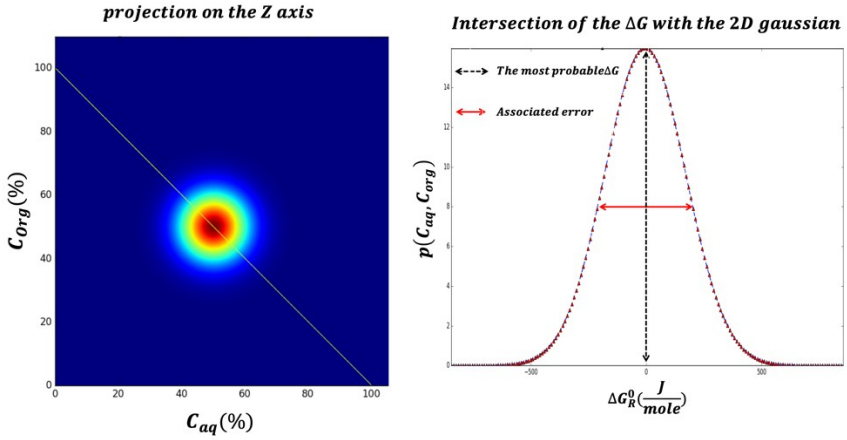

Figure 6 : Sectional view of the Z plane (left) and Intersection curve of the mass conservation plane and two-dimensional Gaussian (right)

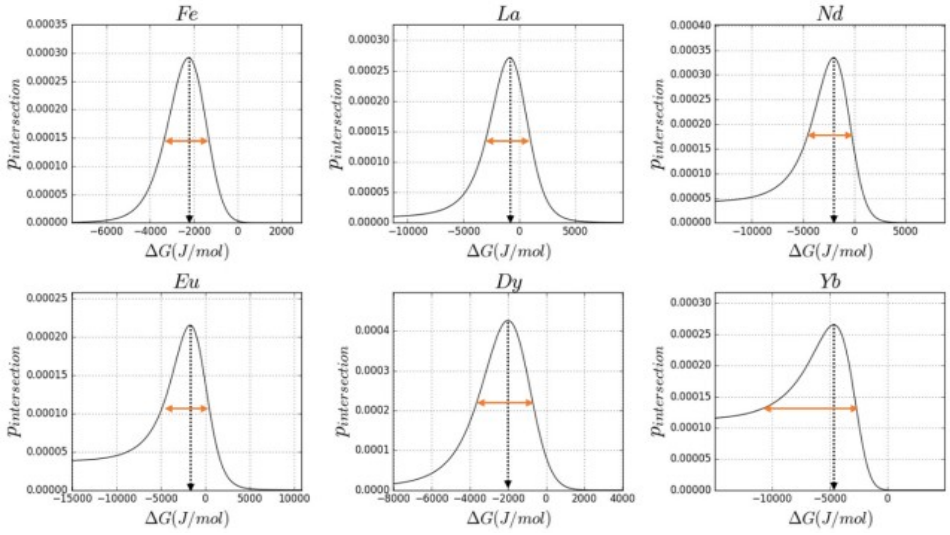

Figure 7: Example of ΔG measurement at maximum probability and associated error defined by half width (Orange arrow). microfluidic extraction point 60 minutes. 50% DMDOHEMA / HDEHP. HNO_3= 3M

The error bars for the ICP measurements correspond to the uncertainty calculated from equation 1. The error in ICP concentrations is estimated by the Error bars of concentrations measured for solution standards. A fixed error of 1% and a proportional error of 3% on the concentration were observed.

$$u_c^2(\Delta G)_{ICP} = \left(\frac{\partial \Delta G}{\partial C_{aq_0}}\right)^2 u^2(C_{aq0}) + \left(\frac{\partial \Delta G}{\partial C_{aq}}\right)^2 u^2(C_{aq}) \qquad \text{Equation 3}$$

$$p(C_{aq}.C_{org}) = \frac{1}{2\pi\,\sigma_{aq}\sigma_{org}} e^{-\frac{1}{2}\left[\left(\frac{C_{aq}-C^{mesure}_{aq}}{\sigma_{aq}}\right)^2 + \left(\frac{C_{org}-C^{mesure}_{org}}{\sigma_{org}}\right)^2\right]} \qquad \text{Equation 4}$$

Where $u_c(\Delta G)_{ICP}$ represents the error on the free energy of transfer of the ions from the aqueous phase to the organic phase, $u(C_{aq0})$ the error on the measurement of the concentration in the initial aqueous phase before extraction and $u(C_{aq})$ after extraction.
In the Figure 8(a) below, we focus on the case where the rare earth elements are well extracted. In this delicate case, the aqueous rare earth concentration is close to zero and therefore the ICP errors on ΔG^0 diverge and tend towards infinity, while they remain acceptable in the case of XRF. In the case where the efficiency of the extraction is moderate (Figure 8 (b)), we notice that the measurement error increases for the XRF, whereas it decreases for the ICP.

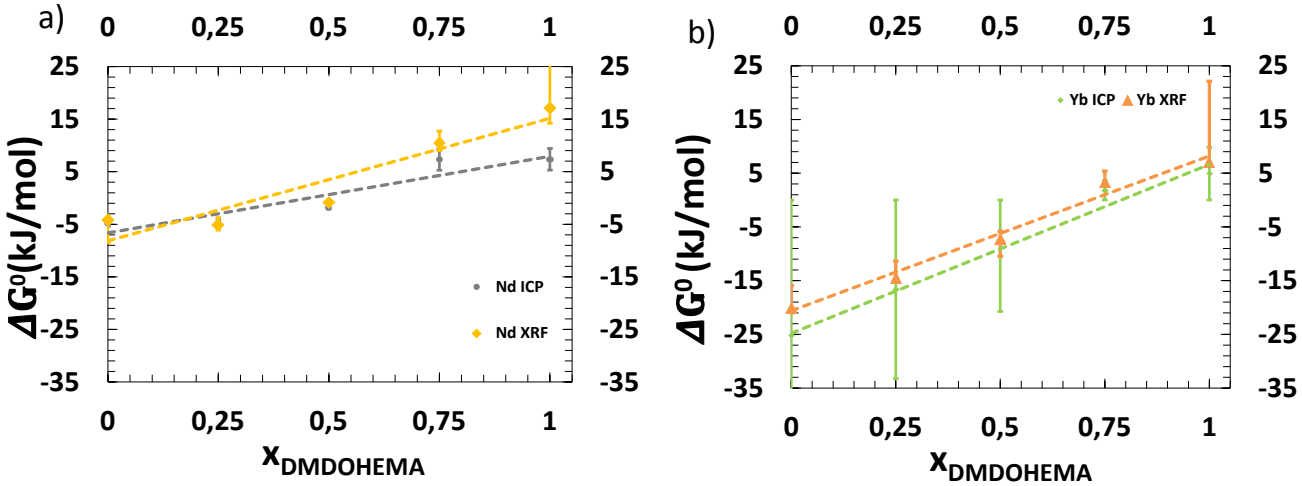

Figure 8: comparison of the free energy of transfer derived from classical Induced Coupled Plasma analysis (ICP) versus the constrained SIMPLEXE method used for exploiting paralel X-ray fluorescence (XRF). Initial organic phase: $[DMDOHEMA]_{tot}$+$[HDEHP]_{tot}$ =0.9M in Isane. Initial aqueous phase: Ln(III) = 10 mM, $[HNO_3]$ = 0.03M, T = 25°C : (a) for neodymium. (b) for ytterbium.

1.6. Comparison microfluidic/literature

Table 5: experimental parameters of the comparative study

Experimental parameters		
Microfluidics (This study)	**J.MULLER** [1]	**J.REY** [2,3]

[HNO_3] (M)	3	1	1
Elements	5 Lanthanides + Fe	Eu with Lithium	Eu
[Elements] (M)	0.01	1E-12	0.05
Extractants	DMDOHEMA HDEHP	DMDOHEMA HDEHP	DMDOHEMA HDEHP
$[Extractant]_{tot}$ (M)	0.9	0.6	0.6

In the study of J. Muller,[7] europium is more extracted than in our measurements. This difference comes from the addition of lithium salts within the aqueous phase which suppresses electrostatic interactions and then modifies the chemical potential without modifying the acidity of the aqueous phase, thus increasing the extraction performance.
In the case of J. Rey *et al.*'s work.[8, 9] the acidity is three times less and europium is five times more concentrated than in our study, respectively. The energy of transfer measures the energy balance between the two extraction phases and does not quantify the extracted concentrations. The initial concentration of ions in the aqueous phase may exceed the capacity of the extractant and the amount of ions in the aqueous phase becomes greater than that in the organic phase. The resulting energy of transfer increases. In the absence of the ionic extractant i.e $x_{DMDOHEMA} = 1$, the free energy of transfer increases in the case of J. Rey *et al.* and this is due to the absence of the electrostatic contribution and the DMDOHEMA is known to extract rare earths at high acidity.

Figure 9 it can also be observed that for all three cases the free energy of transfer can be fitted by a quadratic function in x(1-x), which is equivalent, in a first approximation, to the variation of entropy. The entropic coefficient is smaller in J. Rey's *et al.*, due to the use of lower amount of extractant molecules.

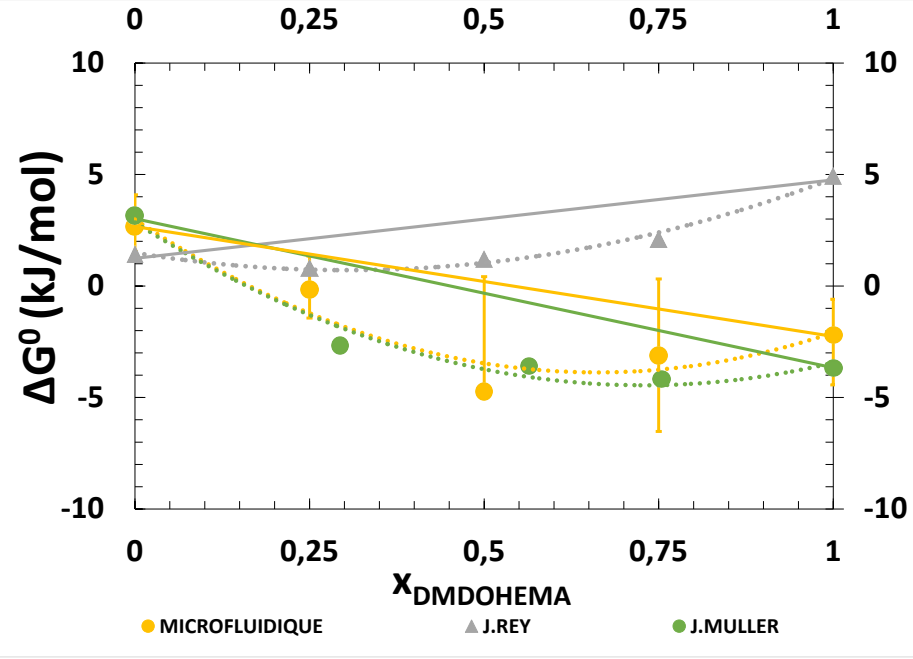

Figure 9: Comparison of the extraction system DMDOHEMA / HDHEP [HNO_3] 3M. XRF. with the data obtained in the literature in similar but different condition : adding 3 M of $Li(NO_3)_3$ in order to kill all electrostatic terms (J. Muller *et al.*)[7] and J. Rey *et al.*[8, 9] for higher load and lower nitric acid concentration. For each case a slight synergy is observed.

1.7. Experimental Data

Table 6: Raw data of the extraction kinetics in microfluidics for the different rare earths and molar fractions with their associated error bars calculated using the Equation 1 for [HNO_3] = 0.03 M.

$X_{DMDOHEMA}$	Contact time (min)	Extraction percentage (%)									
		La	Error bars	Nd	Error bars	Eu	Error bars	Dy	Error bars	Yb	Error bars
0	1	4,2824	0,1285	6,2082	0,3104	20,1388	0,8056	33,7294	1,6865	42,9848	2,1492
	3	6,9690	0,2091	18,0038	0,9002	57,5186	2,3008	72,4248	3,6212	80,2428	4,0121
	10	21,6238	0,6487	37,7579	1,8879	56,0068	2,2403	63,0688	3,1534	80,7529	4,0377
	30	56,5657	1,6970	80,8381	4,0419	93,4210	3,7368	95,6373	4,7819	97,3591	4,8680
	60	61,1046	1,8331	87,1510	4,3576	99,0682	3,9627	99,9404	4,9970	99,9961	4,9998
	120	62,0000	1,8600	87,2000	4,3600	99,7900	3,9916	99,9600	4,9980	99,9900	4,9995
	480	62,3000	1,8690	87,3000	4,3650	99,8000	3,9920	99,9600	4,9980	99,9990	5,0000
0,25	1	3,8546	0,1927	5,8920	0,1768	14,8130	0,7407	14,9541	0,7477	13,0243	0,6512
	3	4,0525	0,2026	7,6753	0,2303	19,9863	0,9993	22,1603	1,1080	24,4433	1,2222
	10	3,0460	0,1523	11,0117	0,3304	27,3083	1,3654	33,9187	1,6959	51,7437	2,5872
	30	30,0000	1,5000	40,1202	1,2036	71,7400	3,5870	96,4845	4,8242	99,4318	4,9716
	60	50,1000	2,5050	61,9803	1,8594	96,3887	4,8194	99,6503	4,9825	99,8779	4,9939
	120	51,0000	2,5500	80,1690	2,4051	97,0000	4,8500	99,6802	4,9840	99,9000	4,9950
	180	52,6000	2,6300	83,9680	2,5190	97,6000	4,8800	99,6959	4,9848	99,9990	5,0000
	480	52,8000	2,6400	84,0000	2,5200	97,8540	4,8927	99,7012	4,9851	99,9999	5,0000
0,5	1	2,7141	0,1357	3,4052	0,1703	10,9796	0,5490	9,4030	0,4702	10,4540	0,4182
	3	2,6380	0,1319	4,0173	0,2009	12,2642	0,6132	9,8113	0,4906	12,3318	0,4933
	10	4,1313	0,2066	8,2249	0,4113	18,9166	0,9458	20,7636	1,0382	34,2530	1,3701
	30	13,7162	0,6858	19,9835	0,9992	34,4338	1,7217	39,6750	1,9838	63,7534	2,5501
	60	45,3699	2,2685	67,3309	3,3666	84,2111	4,2106	93,1214	4,6561	98,5001	3,9400
	120	59,9000	2,9950	80,0000	4,0000	90,0000	4,5000	96,0000	4,8000	99,0000	3,9600
	180	60,0000	3,0000	81,0000	4,0500	91,0000	4,5500	96,6000	4,8300	99,9000	3,9960
	480	60,1000	3,0050	81,6000	4,0800	91,3000	4,5650	96,6600	4,8330	99,9000	3,9960
0,75	1	0,3354	0,0168	0,8328	0,0416	6,3939	0,3197	1,6175	0,0809	0,6950	0,0348
	3	1,8493	0,0925	1,4319	0,0716	8,1974	0,4099	5,4252	0,2713	11,1080	0,5554
	10	2,6036	0,1302	2,4608	0,1230	8,4140	0,4207	17,4575	0,8729	16,1613	0,8081
	30	3,0959	0,1548	4,0306	0,2015	10,8537	0,5427	18,0317	0,9016	24,4190	1,2210
	60	3,1534	0,1577	4,9866	0,2493	11,4208	0,5710	18,3277	0,9164	32,2553	1,6128
	120	4,1258	0,2063	5,0214	0,2511	12,0357	0,6018	18,3565	0,9178	33,6587	1,6829
	180	4,5423	0,2271	5,3480	0,2674	12,3547	0,6177	18,6321	0,9316	34,6570	1,7329
	480	4,5687	0,2284	5,4870	0,2744	12,4587	0,6229	18,6540	0,9327	34,7542	1,7377
1	1	0,9594	0,0395	3,0197	0,0392	3,5746	0,0378	9,1582	0,0384	11,2321	0,0389
	3	1,1501	0,0392	4,1160	0,0390	4,8611	0,0376	10,1930	0,0382	11,2639	0,0389
	10	2,1424	0,0392	4,2000	0,0390	4,8683	0,0376	10,1944	0,0382	11,5129	0,0389
	30	3,1186	0,0388	4,1615	0,0390	5,0936	0,0377	9,9754	0,0381	11,5652	0,0389
	60	3,1602	0,0387	4,8678	0,0389	5,2472	0,0375	11,0910	0,0381	12,1265	0,0388
	120	3,6547	0,1827	4,9651	0,1490	6,2340	0,2494	11,2145	0,5607	12,5478	0,6274
	180	4,0126	0,2006	4,9854	0,1496	6,5478	0,2619	11,2346	0,5617	12,6587	0,6329
	480	4,0265	0,2013	4,9875	0,1496	6,5875	0,2635	11,5475	0,5774	12,6541	0,6327

Table 7: Raw data of the extraction using the standard batch method for the different rare earths and molar fractions with their associated error bars calculated using the Equation 1 for [HNO_3] = 0.03 M.

	Extraction percentage (%)									
$X_{DMDOHEMA}$	La	Error bars	Nd	Error bars	Eu	Error bars	Dy	Error bars	Yb	Error bars
0	60,0147	3,00074	85,98972	4,29949	98,98425	3,95937	99,93925	4,99696	99,99613	2,99988
0.25	52,79691	2,63985	83,28569	4,16428	96,36786	3,85471	99,68158	4,98408	99,8869	2,99661
0.5	43,84442	2,19222	67,48914	3,37446	85,72113	3,42885	92,21282	4,61064	98,14448	2,94433
0.75	3,13736	0,15687	5,92287	0,29614	15,10913	0,60437	18,5808	0,92904	32,53068	0,97592
1	2,53212	0,12661	3,25157	0,16258	4,13303	0,16532	11,65744	0,58287	11,88341	0,3565

Table 8: Raw data of the extraction kinetics in microfluidics for the different rare earths and molar fractions with their associated error bars calculated using the Equation 1 for [HNO_3] = 0.3 M. Data for the molar fraction 0.75 and 1 are not available because a third phase appeared for $x_{DMDOHEMA}$ >0.5

		Extraction percentage (%)									
$X_{DMDOHEMA}$	Contact time (min)	La	Error bars	Nd	Error bars	Eu	Error bars	Dy	Error bars	Yb	Error bars
0	1	2,4994	0,125	6,4858	0,3243	1,0967	0,0548	3,1883	0,1594	20,52	1,026
	3	2,5586	0,1279	3,3733	0,1687	10,025	0,5012	7,5967	0,3798	54,706	2,7353
	10	3,4195	0,171	4,0786	0,2039	10,581	0,529	12,583	0,6291	86,423	4,3212
	30	3,7835	0,1892	5,6277	0,2814	11,893	0,5947	17,739	0,887	90,414	4,5207
	60	3,8387	0,1919	5,8208	0,291	11,581	0,5791	18,228	0,9114	90,746	4,5373
0.25	1	9,6058	0,0365	10,002	0,0375	11,161	0,0396	14,616	0,0375	17,84	0,892
	3	13,388	0,0358	16,965	0,0362	16,068	0,0386	31,034	0,0347	35,235	1,7618
	10	18,552	0,0349	28,652	0,0342	35,621	0,0352	47,411	0,0323	66,217	3,3109
	30	29,24	0,0332	41,822	0,0322	50,16	0,0331	61,868	0,0306	80,739	4,0369
	60	30,179	0,033	41,864	0,0322	50,419	0,033	62,23	0,0305	81,494	4,0747
0.5	1	13,29	0,6645	16,749	0,8375	16,859	0,843	17,205	0,8603	12,15	0,6075
	3	22,199	1,11	30,467	1,5233	31,941	1,597	34,342	1,7171	34,613	1,7307
	10	53,24	2,662	66,204	3,3102	68,19	3,4095	70,969	3,5484	77,272	3,8636
	30	75,387	3,7694	82,409	4,1204	82,896	4,1448	84,571	4,2286	86,991	4,3495
	60	77,051	3,8526	82,904	4,1452	83,181	4,159	84,824	4,2412	87,328	4,3664

Table 9: Raw data of the extraction using the standard batch method for the different rare earths and molar fractions with their associated error bars calculated using the Equation 1 for [HNO_3] = 0.3 M. Data for the molar fraction 0.75 and 1 are not available because a third phase appeared for $x_{DMDOHEMA}$ >0.5

	Extraction percentage (%)									
$X_{DMDOHEMA}$	La	Error bars	Nd	Error bars	Eu	Error bars	Dy	Error bars	Yb	Error bars
0	0,76975	0,03079	0,39093	0,01955	3,4664	0,17332	17,09268	0,68371	89,02274	4,45114
0.25	30,09829	1,20393	41,86538	2,09322	49,9	2,495	53,87177	2,15487	80,05065	4,00253
0.5	75,43673	3,01747	81,49729	4,07486	81,87999	4,094	83,19076	3,32763	86,89839	4,34492

Table 10: Raw data of the extraction kinetics in microfluidics for the different rare earths and molar fractions with their associated error bars calculated using the Equation 1 for [HNO_3] = 3 M.

		Extraction percentage (%)									
$x_{DMDOHEMA}$	Contact time (min)	La	Error bars	Nd	Error bars	Eu	Error bars	Dy	Error bars	Yb	Error bars
0	1	1,4121	0,0989	5,6966	0,3418	9,3587	0,4679	3,9568	0,1978	34,026	1,7013
	3	2,1183	0,1483	6,5446	0,3927	9,8306	0,4915	7,8481	0,3924	65,361	3,268
	10	2,137	0,1496	6,7835	0,407	10,944	0,5472	20,621	1,031	86,905	4,3453
	30	3,1411	0,2199	7,9107	0,4746	12,576	0,6288	25,924	1,2962	88,073	4,4036
	60	3,3047	0,2313	7,989	0,4793	12,784	0,6392	26,007	1,3003	88,509	4,4255
0.25	1	10,177	0,5088	8,8973	0,4449	5,5025	0,2751	7,0383	0,3519	9,1822	0,4591
	3	12,528	0,6264	15,36	0,768	13,822	0,6911	17,999	0,8999	28,567	1,4283
	10	18,827	0,9413	25,321	1,266	27,418	1,3709	38,136	1,9068	73,533	3,6766
	30	35,949	1,7974	41,52	2,076	46,484	2,3242	61,479	3,0739	87,888	4,3944
	60	36,309	1,8154	42,724	2,1362	47,177	2,3589	61,505	3,0752	88,233	4,4116
0.5	1	17,487	0,8744	20,212	1,0106	17,058	0,8529	18,898	0,9449	10,718	0,5359
	3	28,404	1,4202	34,066	1,7033	30,739	1,537	33,024	1,6512	26,82	1,341
	10	57,747	2,8874	65,883	3,2942	62,674	3,1337	64,972	3,2486	62,869	3,1434
	30	90,585	4,5292	91,247	4,5624	92,46	4,623	92,218	4,6109	93,556	4,6778
	60	90,949	4,5475	91,416	4,5708	93,579	4,679	93,608	4,6804	94,128	4,7064
0.75	1	13,554	0,6777	14,927	0,7464	11,635	0,5818	12,624	0,6312	4,6385	0,2319
	3	17,284	0,8642	21,267	1,0634	26,153	1,3076	25,444	1,2722	40,6	2,03
	10	42,198	2,1099	58,795	2,9397	68,682	3,4341	69,757	3,4879	84,432	4,2216
	30	81,794	4,0897	83,36	4,168	85,071	4,2536	89,095	4,4548	88,649	4,4325
	60	81,933	4,0966	83,981	4,199	85,531	4,2765	89,776	4,4888	89,861	4,493
1	1	17,289	0,0358	18,093	0,036	13,75	0,0399	14,036	0,0361	4,3848	0,0411
	3	38,242	0,0325	41,096	0,0323	33,041	0,0364	29,914	0,0334	11,746	0,0396
	10	70,984	0,0288	74,287	0,0287	64,988	0,032	57,081	0,0298	50,483	0,0351
	30	80,744	0,0278	81,291	0,028	85,518	0,0306	88,969	0,0277	88,675	0,03
	60	80,744	0,0279	81,497	0,0281	85,535	0,0305	88,897	0,0275	88,952	0,0299

Table 11: Raw data of the extraction using the standard batch method for the different rare earths and molar fractions with their associated error bars calculated using the Equation 1 for [HNO_3] = 3 M.

	Extraction percentage (%)									
$X_{DMDOHEMA}$	La	Error bars	Nd	Error bars	Eu	Error bars	Dy	Error bars	Yb	Error bars
0	3,3047	0,16523	8,124	0,4062	12,45139	0,62257	27,45782	1,37289	88,51842	4,42592
0.25	36,54646	1,82732	42,863	2,14315	47,74056	2,38703	62,80684	3,14034	88,09525	4,40476
0.5	90,88206	4,5441	92,25455	4,61273	93,14434	4,65722	92,64164	4,63208	93,09495	4,65475
0.75	81,71054	4,08553	84,0924	4,20462	85,20958	4,26048	88,49983	4,42499	90,03111	4,50156
1	80,76576	4,03829	81,01432	4,05072	85,91218	4,29561	88,25809	4,4129	89,15482	4,45774

Table 12: Free energies of transfer ΔG^0 (kJ/mol) for different lanthanides and molar fractions with their associated error bars (ΔG^0err.L and ΔG^0err.R) calculated using the developed constrained SIMPLEXE method[6] for $[HNO_3]$ = 0.03 M.

Elts	La			Nd			Eu			Dy			Yb		
$X_{DMDOHEMA}$	ΔG^0 (kJ/mol)	$\Delta G^0_{err.L}$	$\Delta G^0_{err.R}$	ΔG^0 (kJ/mol)	$\Delta G^0_{err.L}$	$\Delta G^0_{err.R}$	ΔG^0 (kJ/mol)	$\Delta G^0_{err.L}$	$\Delta G^0_{err.R}$	ΔG^0 (kJ/mol)	$\Delta G^0_{err.L}$	$\Delta G^0_{err.R}$	ΔG^0 (kJ/mol)	$\Delta G^0_{err.L}$	$\Delta G^0_{err.R}$
0	-0.6680	0.5198	0.5655	-4.1829	0.8057	4.3097	-9.9110	2.9342	2.4003	-15.6467	3.8522	0.4884	-20.0000	4.0841	0.9627
0.25	-1.2974	0.5848	0.7280	-5.1214	1.3894	1.0079	-8.1214	2.5547	2.9969	-10.0993	2.2060	2.3376	-14.3851	3.0514	0.9090
0.5	1.6103	0.5574	0.4607	-0.8579	0.5797	0.4981	-3.7995	1.4389	0.5481	-4.8559	1.1327	0.0036	-7.1800	1.3908	3.3107
0.75	17.1120	15.0000	2.7437	10.5411	2.1903	1.5618	8.0747	3.0124	0.9733	7.9426	3.0565	0.9459	3.3885	2.0042	0.7427
1	17.1120	15.0000	3.1006	17.1120	15.0000	2.9145	17.1120	15.0000	3.5421	17.1120	15.0000	3.2000	7.1120	15.0000	0.1147

Table 13: Free energies of transfer ΔG^0 (kJ/mol) for different lanthanides and molar fractions with their associated error bars (ΔG^0err.L and ΔG^0err.R) calculated using the developed constrained SIMPLEXE method[6] for $[HNO_3]$ = 0.3 M.

Elts	La			Nd			Eu			Dy			Yb		
$X_{DMDOHEMA}$	ΔG^0 (kJ/mol)	$\Delta G^0_{err.L}$	$\Delta G^0_{err.R}$	ΔG^0 (kJ/mol)	$\Delta G^0_{err.L}$	$\Delta G^0_{err.R}$	ΔG^0 (kJ/mol)	$\Delta G^0_{err.L}$	$\Delta G^0_{err.R}$	ΔG^0 (kJ/mol)	$\Delta G^0_{err.L}$	$\Delta G^0_{err.R}$	ΔG^0 (kJ/mol)	$\Delta G^0_{err.L}$	$\Delta G^0_{err.R}$
0	4.2017	1.0487	0.5453	2.9243	0.5522	0.4085	2.0056	0.4407	0.3611	1.9132	0.6776	0.5153	-3.8762	0.5923	1.1933
0.25	1.1814	0.5536	0.4765	-0.1487	0.5140	0.5241	-0.9428	0.5673	0.6513	-1.2974	0.4556	0.5286	-4.6662	0.6613	2.0873
0.5	-3.0000	0.6289	0.7587	-3.9000	0.6634	1.0480	-3.9600	0.8552	1.3833	-4.7800	0.4566	0.5733	-4.8000	0.5485	0.9066

Table 14: Free energies of transfer ΔG^0 (kJ/mol) for different lanthanides and molar fractions with their associated error bars (ΔG^0err.L and ΔG^0err.R) calculated using the developed constrained SIMPLEXE method[6] for $[HNO_3]$ = 3 M.

Elts	La			Nd			Eu			Dy			Yb		
$X_{DMDOHEMA}$	ΔG^0 (kJ/mol)	$\Delta G^0_{err.L}$	$\Delta G^0_{err.R}$	ΔG^0 (kJ/mol)	$\Delta G^0_{err.L}$	$\Delta G^0_{err.R}$	ΔG^0 (kJ/mol)	$\Delta G^0_{err.L}$	$\Delta G^0_{err.R}$	ΔG^0 (kJ/mol)	$\Delta G^0_{err.L}$	$\Delta G^0_{err.R}$	ΔG^0 (kJ/mol)	$\Delta G^0_{err.L}$	$\Delta G^0_{err.R}$
0	5.3623	3.0076	0.6579	3.6903	0.6706	0.4419	2.6693	0.4736	0.3713	1.9247	0.6390	0.4925	-5.2568	0.7261	3.9517
0.25	2.1944	0.5898	0.4479	0.7692	0.4591	0.4221	-0.1696	0.5031	0.4222	-0.9325	0.4266	0.4774	-4.8211	0.6731	2.6131
0.5	-3.8506	1.6253	0.2763	-4.0289	1.2835	0.2270	-4.7322	1.7165	0.0449	-4.9940	1.4420	0.4346	-5.6447	0.9831	1.6321
0.75	-2.2678	1.0702	0.2520	-2.8292	0.9200	0.0091	-3.1111	1.1429	1.1381	-3.6824	0.9337	0.1233	-3.7761	0.3382	2.8333
1	-1.5445	0.1039	1.6870	-1.9846	0.3178	5.0425	-2.1944	0.5323	0.7473	-3.2976	0.1473	1.1732	-3.0389	0.0610	1.6786

Table 15: Free energies of transfer ΔG^0 (kJ/mol) for different lanthanides and temperatures. [HNO3] = 3 M and $x_{DMDOHEMA}$ = 0.5

	T=15°C			T=25°C			T=35°C		
Elts	ΔG^0 (kJ/mol)	$\Delta G^0_{err.L}$	$\Delta G^0_{err.R}$	ΔG^0 (kJ/mol)	$\Delta G^0_{err.L}$	$\Delta G^0_{err.R}$	ΔG^0 (kJ/mol)	$\Delta G^0_{err.L}$	$\Delta G^0_{err.R}$
La	-1.2234	0.5269	0.6279	-0.3076	1.1569	0.5424	4.8211	0.6885	0.7768
Nd	-2.0789	0.6250	0.9682	-0.7591	0.5295	0.3761	3.4192	1.0098	4.8700

Eu	-2.3523	0.6296	0.8936	-1.5665	0.4730	0.3576	3.0784	1.0298	4.7701
Dy	-4.8648	0.4551	0.6717	-1.8675	0.3003	0.2987	0.2281	7.3974	4.0106
Yb	-7.3477	1.0549	3.2548	-5.2054	0.3714	0.4830	-2.6044	7.9911	3.4169

Table 16: Entropy-Enthalpy for the different lanthanides tested and their three physical quantities: ionic radius. ionic volume and surface charge density.

Element	Ionic radius (nm)	Ionic volume (nm^3)	Surface charge density (e/nm^2)	ΔH(kJ/mol)	TΔS(kJ/mol)
La	0.105	0.0076	21.6537	-89.1120	-87.0876
Nd	0.099	0.0064	24.3580	-81.7690	-79.2153
Eu	0.095	0.006	26.4523	-81.2380	-78.2414
Dy	0.091	0.0051	28.8289	-78.0900	-73.3745
Yb	0.087	0.0042	31.5408	-75.7640	-68.3405

1. G. B. Dantzig, *Programming in a Linear Structure.* , Washington DC., 1948.
2. H. Abdi, *Wiley Interdisciplinary Reviews-Computational Statistics*, 2010, **2**, 97-106.
3. K. H. Angeyo, S. Gari, A. O. Mustapha and J. M. Mangala, *Applied Radiation and Isotopes*, 2012, **70**, 2596-2601.
4. D. Kirsanov, V. Panchuk, M. Agafonova-Moroz, M. Khaydukova, A. Lumpov, V. Semenov and A. Legin, *Analyst*, 2014, **139**, 4303-4309.
5. D. Kirsanov, V. Panchuk, A. Goydenko, M. Khaydukova, V. Semenov and A. Legin, *Spectrochimica Acta Part B-Atomic Spectroscopy*, 2015, **113**, 126-131.
6. C. Penisson, Ph. D., Université de Grenoble Alpes, 2018.
7. J. Muller, PhD Thesis, Université Pierre et Marie Curie-Paris VI, 2012.
8. J. Rey, M. Bley, J.-F. Dufrêche, S. Gourdin, S. Pellet-Rostaing, T. Zemb and S. Dourdain, *Langmuir*, 2017, **33**, 13168-13179.
9. J. Rey, S. Dourdain, J.-F. Dufrêche, L. Berthon, J. M. Muller, S. Pellet-Rostaing and T. Zemb, *Langmuir*, 2016, **32**, 13095-13105.